Shear stress augments mitochondrial ATP generation that triggers ATP release and Ca^{2+} signaling in vascular endothelial cells

Kimiko Yamamoto[1]*, Hiromi Imamura[2], Joji Ando[3]*

[1]Laboratory of System Physiology, Department of Biomedical Engineering, Graduate School of Medicine, University of Tokyo, Tokyo113-0033, Japan.

[2]Laboratory of Functional Biology, Graduate School of Biostudies, Kyoto University, Kyoto 606-8501, Japan

[3]Laboratory of Biomedical Engineering, School of Medicine, Dokkyo Medical University, Tochigi 321-0293, Japan

*These authors contributed equally to this work.

Correspondence should be addressed to K.Y (k-yamamoto@umin.ac.jp)

ABSTRACT

Vascular endothelial cells (ECs) sense and transduce hemodynamic shear stress into intracellular biochemical signals, and Ca^{2+} signaling plays a critical role in this mechanotransduction, i.e., the ECs release ATP in the caveolae in response to shear stress, and in turn, the released ATP activates the P2 purinoceptors, which results in an influx into the cells of extracellular Ca^{2+}. However, the mechanism by which the shear stress evokes ATP release remains unclear. Here we demonstrate that the cellular mitochondria play a critical role in this process. Cultured human pulmonary artery ECs were exposed to controlled levels of shear stress in a flow-loading device and the changes in the mitochondrial ATP levels were examined by real-time imaging using a fluorescence resonance energy transfer-based ATP biosensor. Immediately upon the exposure of the cells to flow, the mitochondrial ATP levels increased, which was both reversible and dependent on the shear stress intensity. Inhibitors of the mitochondrial electron transport chain and ATP synthase, as well as knockdown of caveolin-1, a major structural protein of the caveolae, abolished the shear-stress-induced mitochondrial ATP generation, resulting in the loss of the ATP release and influx of Ca^{2+} into the cells. These results suggest the novel role of the mitochondria in transducing the shear stress into ATP generation: the ATP generation leads to ATP release in the caveolae, triggering purinergic Ca^{2+} signaling. Thus, exposure of ECs to shear stress seems to activate mitochondrial ATP generation through caveola- or caveolin-1-mediated mechanisms.

Key words: endothelial cells; mitochondria; shear stress; ATP; calcium signaling

New & Noteworthy

The mechanism how vascular endothelial cells sense shear stress generated by blood flow and transduce it into functional responses remains unclear. Real-time imaging of mitochondrial ATP demonstrates the novel role of endothelial mitochondria as mechanosignaling organelles that are able to transduce shear stress into ATP generation, triggering ATP release and purinoceptor-mediated Ca^{2+} signaling within the cells.

INTRODUCTION

The endothelial cells (ECs) that line the lumens of blood vessels are constantly exposed to a fluid dynamic force, the shear stress generated by the flow of blood. The ECs sense this shear stress and transduce it into intracellular biochemical signals, resulting in changes in the morphology, functions, and gene expression profiles of the cells (13). These EC mechanoresponses are critical for the homeostasis of the circulatory system, and their impairment can lead to the development of various vascular diseases, including hypertension, aneurysm, thrombosis, and atherosclerosis (5, 11, 40).

A large number of studies have focused on clarifying the mechanisms of EC mechanotransduction. A unique feature found to be associated with exposure of the cells to shear stress is the almost simultaneous activation of multiple intracellular signal transduction pathways through various membrane molecules and microdomains (4). Ca^{2+} signaling mediated by purinergic receptors has been shown to serve as one of these shear stress mechanotransduction pathways (3, 35). When exposed to shear stress, ECs rapidly release intrinsic ATP; this, in turn, activates P2X4 and P2Y2 receptors, triggering the influx of extracellular Ca^{2+} and Ca^{2+} release from intracellular Ca^{2+} stores. The resulting increase in the cytoplasmic Ca^{2+} concentration results in the augmented production of nitric oxide, which plays a crucial role in the regulation of blood pressure, blood flow-dependent vasodilation, and vascular remodeling in tissues (40).

In recent years, we have developed a novel chemiluminescence method for imaging cell-surface ATP. This has demonstrated that shear stress causes a focal release of ATP in the caveolae-rich regions of EC plasma membranes, with concentrations exceeding 10 μM (37). Co-imaging of ATP and Ca^{2+} showed that the Ca^{2+} influx started at the site of the focal ATP release, with the increase in the cytoplasmic Ca^{2+}concentration propagating through the entire cell as a Ca^{2+} wave. However, it remains unclear how exposure of the cells to shear stress evokes the release of ATP.

In the present study, we investigated possible roles of the mitochondria in the ATP release. We used a fluorescence resonance energy transfer (FRET)-based ATP biosensor (20) to visualize the ATP inside the mitochondria of cultured human pulmonary aortic ECs (HPAECs), and analyzed the changes in mitochondrial ATP generation following exposure to shear stress. We also examined how membrane microdomain caveolae (2) are involved in the mitochondrial responses to shear stress.

MATERIALS AND METHODS

Cell culture. The HPAECs were purchased from Lonza Walkersville Inc. (Product code:cc-2530) and grown in M199 supplemented with 15% fetal bovine serum, 2 mM L-glutamine (Gibco), 50 μg/ml heparin, and 30 μg/ml EC growth factor (Becton Dickinson) in a 1% gelatin-coated tissue culture flask. The cells used in the experiments in this study were in the 7th and 10th passages. All experiments were approved by the Ethics Committee of The University of Tokyo, Graduate School of Medicine.

Shear stress experiments. Cells were subjected to controlled levels of laminar shear stress in a parallel plate-type flow-loading device (FCS2, Bioptechs), as previously described (41). Briefly, the flow chamber consisted of a 1 %-gelatin-coated cover glass with the cultured cells on one side, and a second, parallel, glass plate held 200 μm apart from the first by a Teflon™ gasket. The medium was perfused with a roller/tube pump, and the entire closed circuit was maintained at exactly 37 °C. The intensity of the shear stress (τ, dynes/cm^2) acting on the EC layer was calculated from the formula, $\tau = 6\mu Q/a^2 b$, where μ is the viscosity of the perfusate (poise), Q is the flow volume (mL/s), and *a* and *b* are the cross-sectional dimensions of the flow path (cm).

Imaging of mitochondrial ATP. The mitochondrial ATP was imaged using a FRET-based ATeam (adenosine 5'-triphosphate indicator based on epsilon subunit for analytical measurements) biosensor targeted at the mitochondrial matrix (mitAT1.03). The cDNA of mitAT1.03 was ligated and cloned into the *Sal*I/*Not*I sites of a pAd-CMV-V5-DEST Gateway Vector (Thermo Fisher Scientific), and the adenovirus vector containing mitAT1.03 cDNA (Ad-mitAT1.03) was constructed as described previously (20). Cultured HPAECs were infected with 50 pfu/cell of Ad-mitAT1.03.

Three to five days after Ad-mitAT1.03 infection, the HPAECs (maintained at 37°C) were imaged on an ECLIPSE Ti-E inverted microscope (Nikon) with 60× and 100× Apo TIRF oil objectives (1.49 numerical aperture (NA)) using a water-cooling electron multiplier CCD camera (ImagEM C9100-13, Hamamatsu), controlled by HCImage software version 4.3 (Hamamatsu). The dual-emission ratio imaging of mitAT1.03 used an FF01-427/10 excitation filter (Semrock), an FF458-Di01 dichroic mirror, and a Dual View Multichannel Imaging System (DV2, Photometrics) equipped with two emission filters (FF01-483/32 for CFP and FF01-542/27 for YFP). The images were analyzed by using MetaMorph software program version 7.7 (Molecular Devices).

Characterization of AT1.03 protein. The ATP sensitivity of ATeam (AT1.03) was examined in vitro. The concentration of purified AT1.03 protein was adjusted with buffer (comprising 50 mM MOPS-KOH [pH 7.3], 50 mM KCl, 0.5 mM $MgCl_2$, and 0.05% Triton X-100) so that the fluorescent intensity of CFP was equivalent to that observed in HPAECs using the same microscope system. The changes in CFP and YFP emissions for different concentration of ATP magnesium salt (Mg-ATP) were measured at 37°C, and the YFP/CFP emission ratios were calculated.

Measurement of Extracellular ATP. The ATP released by the HPAECs was measured by means of a luciferin-luciferase assay, as previously described (41). The cells were exposed to laminar flow in a flow chamber. The perfusate flowing out of the chamber was collected every 10 s, and 100 μL was

applied to the ATP assay system (Toyo Ink, Tokyo). The ATP assay mixture (luciferase, D-luciferin, and bovine serum albumin) was injected into each sample, and the relative light intensity was recorded for 10 s in a Wallac 1420 ARVO SX multilabel counter (Perkin Elmer). A calibration curve for ATP concentrations was obtained for each experiment by using the same batch of luciferin-luciferase reagents.

Immunohistochemistry. Cells were fixed with 4% paraformaldehyde (Sigma) and maintained in 1% normal bovine serum albumin (Sigma) to block nonspecific protein binding sites. The cells were incubated with rabbit anti-caveolin-1 polyclonal antibody (BD Transduction Laboratories); after washing they were incubated with Alexa Fluor 488 goat anti-rabbit IgG (Thermo Fisher Scientific) at a 1:500 dilution. The stained cells were photographed through a confocal fluorescence microscope (Leica), and the images were imported into Adobe Photoshop as TIFFs for figure assembly.

Ca^{2+} measurement. Cells were loaded with the Ca^{2+}-sensitive dye Fluo-4-acetoxymethyl ester (5 μM; Dojindo) and placed in the FCS2 flow chamber (Bioptechs) on the stage of an ECLIPSE Ti-E inverted microscope (Nikon). The fluo-4 was excited with light that passed through a 490-nm band-pass filter (Lambda DG-4), and the emitted light was guided through a 510-nm band-pass filter to a water-cooling electron multiplier CCD camera (ImagEM C9100-13, Hamamatsu). Fluorescence intensity is a reflection of the intracellular Ca^{2+} concentration. The Ca^{2+} images were acquired sequentially as full-frame images (512×512 pixels) with an exposure period of 30 ms. The images were analyzed by using HCImage software version 4.3 (Hamamatsu).

Small-interfering RNA preparation and transfection. Targeted siRNA was used to knock down caveolin-1 expression in HPAECs as described previously (37). A DNA fragment flanked by the *Bam* HI and *Hin*d III sites was synthesized; this contained the sense target sequence corresponding to bases 167-185 from the open reading frame of the human caveolin-1 (GenBank accession number NM_001753; 5'-CTAAACACCTCAACGATGA-3'), the hairpin loop sequence 5'-CTGTGAAGCCACAGATGGG-3', and the antisense target sequence 5'-TCATCGTTGAGGTGTTTAG-3'. The fragment was inserted between the human U6 promoter and the terminator sequences of pBAsi-hU6 (Takara) to generate a stem-loop type of siRNA in the transfected cells. The randomized sequence 5'-TAACATGAACCACGACTAC-3' was used to construct the vector for a negative control (scrambled siRNA). The HPAECs were treated with the construct using Lipofectamine 2000 (Invitrogen) as the transfection reagent. The experiments were conducted 48 h after transfection.

Statistical analysis. The results are presented as the mean ± SD. Statistical significance was evaluated by an ANOVA with the Bonferonni's adjustment applied to the results of post hoc *t* tests. The statistical analysis was performed with SPSS software (SPSS Inc). A *P* value of < 0.05 was regarded as being statistically significant.

RESULTS

Shear stress resulted in rapid augmentation of mitochondrial ATP generation. To monitor changes in the mitochondrial ATP levels, we used a genetically encoded FRET-based ATP biosensor that targeted mitochondrial matrix mitAT1.03. The localization of mitAT1.03 coincided precisely with the mitochondria, as was shown by live-cell imaging using the mitochondrion-selective dye MitoTracker (Fig. 1A). When the ECs were treated with oligomycin, an inhibitor of ATP synthase, the fluorescence of mitAT1.03 yellow fluorescent protein (YFP) decreased, and the fluorescence of cyan fluorescent protein (CFP) increased, thereby reducing the YFP/CFP ratio; this indicated a decrease in mitochondrial ATP generation (Fig. 1B). In contrast, the fluorescence of mitAT1.03 was not affected by treatment of the cells with 2-deoxy-D-glucose (2-DG), an inhibitor of cytosolic glycolysis. An in vitro examination of the ATP sensitivity of purified AT1.03 showed a clear correlation between the YFP/CFP ratio and ATP concentration in the range of 0-10 mM (Fig. 1C). Oligomycin had no effect on the ATP sensitivity of purified AT1.03. These findings indicated that AT1.03 enabled real-time and quantitative observation of the mitochondrial ATP levels.

HPAECs were exposed to controlled levels of shear stress in a flow-loading apparatus and changes in mitochondrial ATP levels were examined. Pseudocolor images of the YFP/CFP ratio showed increased ATP levels over the entire mitochondria when the cells were exposed to shear stress (Fig. 2A). A rough estimate using the correlation curve between the YFP/CFP ratio and ATP concentration suggested that the ATP levels had approximately doubled. The changes in ATP levels over time were quantified by defining regions of interest in the mitochondria. The ATP level increased immediately after exposure of the cells to shear stress (see Supplementary Video 1); this level was maintained throughout the exposure to shear stress and then decreased after the shear stress ceased.

The mitochondrial ATP responses to shear stress were reversible and dose-dependent. When the shear stress was applied repeatedly, the ATP levels in the mitochondria increased repeatedly in response, indicating that the mitochondrial response was reversible (Fig. 2B). When the ECs were exposed to shear stresses at different intensities from 3 to 8 dynes/cm^2, the ATP levels increased in a dose-dependent manner (Fig. 2D, E). In the flow-loading experiments, the ECs were subjected not only to shear stress but also to pressure that exerts a compressive force on the cells. To examine whether the pressure affected the mitochondrial ATP levels, we exposed the ECs to hydrostatic

pressure under a no-flow condition. The hydrostatic pressure alone had no effect on the ATP levels, but when the same cells were exposed to flow in addition to the pressure, the ATP levels clearly increased (Fig. 2C). These findings indicated that the flow-induced increase in mitochondrial ATP generation was attributable to the shear stress and not the pressure to which the cells were exposed.

Shear tress activated the mitochondrial oxidative phosphorylation. Prior to exposure to shear stress, ECs were treated with one of three inhibitors: oligomycin, an ATP synthase inhibitor; carbonyl cyanide m-chlorophenylhydrazone (CCCP), a mitochondrial oxidative phosphorylation uncoupler; or rotenone, an inhibitor of mitochondrial electron transport. All three inhibitors abolished the shear-stress-induced mitochondrial ATP generation in the ECs (Fig. 3A). In contrast, treatment of the cells with the glycolysis inhibitor 2-DG had no such effect. These findings indicate that exposure of ECs to shear stress increased mitochondrial ATP generation by activating the mitochondrial oxidative phosphorylation. Neither addition of EGTA to culture media, which removes extracellular Ca^{2+}, nor treatment of ECs with MitoTEMPOL, which inactivates mitochondrial reactive oxygen species (ROS), exerted any influence on the ATP generation. These findings indicate that the influx of extracellular Ca^{2+} and the ROS produced by mitochondria do not play a part in the shear-stress-induced mitochondrial ATP generation.

Mitochondria were the major source of the ATP released by the ECs in response to shear stress. HPAECs were exposed to shear stress and changes in ATP concentration were measured biochemically in a portion of the perfusate, as described in the Methods section. Exposure of the ECs to shear stress significantly increased the amount of ATP released from the cells (Fig. 3B), which was in good agreement with data obtained in our previous studies (41). The shear-stress-induced ATP release was suppressed by markedly treatment of ECs with oligomycin, CCCP, or rotenone, but treatment of the cells with 2-DG, EGTA and MitoTEMPOL had no effect on the ATP release. These findings indicated that the mitochondrial ATP generation plays a crucial role in the shear-stress-induced ATP release from the cells.

Caveolae were implicated in shear stress-induced mitochondrial ATP generation. HPAECs are rich in caveolae, which are small flask-shaped invaginations of the cell membranes. Fluorescence microscopy using MitoTracker and an antibody against caveolin-1, a major structural protein of caveolae, showed that the caveolae were concentrated at specific areas of the edge of the cell where the mitochondria were located in close proximity (Fig. 4A). Treatment of cells with small interfering RNA (siRNA) of caveolin-1 completely abolished the expression of caveolin-1, indicating destruction of the caveolae, but had no significant effect on the morphology and distribution of the mitochondria. Because

caveolin-1 knockdown with its siRNA significantly inhibited the shear stress-induced ATP release (Fig. 3B), we investigated whether the caveolae or caveolin-1 could be implicated in the shear stress-induced mitochondrial ATP generation. Shear stress-induced mitochondrial ATP generation was not markedly observed in the cells transfected with the caveolin-1 siRNA, in clear contrast to the control cells transfected with the caveolin-1 scrambled siRNA (Fig. 4B). These findings indicated that the caveola or caveolin-1 had a critical role in shear stress-induced mitochondrial ATP generation.

Mitochondrial ATP generation triggered shear stress-mediated Ca^{2+} signaling. ECs were subjected to shear stress and changes in the intracellular Ca^{2+} concentrations ($[Ca^{2+}]_i$) were monitored using the Ca^{2+}-sensitive dye Fluo-4. Shear stress evoked a rapid increase in $[Ca^{2+}]_i$ in the cells treated with the caveolin-1 scrambled siRNA; when the shear stress was terminated, the $[Ca^{2+}]_i$ returned to its basal level (Fig. 4C). This Ca^{2+} response to shear stress did not occur in the cells treated with the caveolin-1 siRNA. Blockage of mitochondrial ATP generation with oligomycin, CCCP, or rotenone abolished the shear stress-mediated Ca^{2+} response. The Ca^{2+} response was blocked by EGTA, but not by MitoTEMPOL, indicating that the Ca^{2+} response is due to the influx of extracellular Ca^{2+} into the cells and that ROS produced by mitochondria do not play a part in the Ca^{2+} responses. These findings indicate the following order of events: mitochondrial ATP generation occurred in response to shear stress, followed by release of the ATP, which induced an increase in the $[Ca^{2+}]_i$ via the influx of extracellular Ca^{2+}.

DISCUSSION

We used the mitochondria-targeting ATP biosensor mitAT1.03 for real-time imaging of mitochondrial ATP generation in cultured ECs under various flow conditions. The ECs rapidly responded to flow with a marked increase in the generation of ATP by the mitochondrial. The mitochondrial response was reversible and dependent on the intensity of shear stress. In recent years, it has been demonstrated that shear stress affects the morphology and functions of the endothelial mitochondria (30). For example, when human umbilical vein ECs were exposed to shear stress for 36 h, mitochondrial biogenesis increased according to the shear stress intensity, resulting in an increase in the number of mitochondria in the cell (23). Exposure of porcine aortic ECs to shear stress for 48 h increased their mitochondrial membrane potential and intracellular ATP levels (24). In bovine aortic ECs, shear stress first induced a dynamic change in the morphology of the mitochondria, including fragmentation and fission, followed by a decrease in the respiration rate and an increase in the generation of reactive oxygen species (ROS) (9). On the other hand, there is also a report of exposure to shear stress not causing any significant morphological changes in the EC mitochondria (18). Furthermore, shear stress increases the intracellular Ca^{2+} concentrations in the ECs, which leads to NO production; these responses have

been shown to secondarily modulate the mitochondrial bioenergetics and ROS production in the cells (21, 33). All of these findings represent relatively long-term effects of shear stress on the mitochondria. In contrast, the present study demonstrated the real-time effect of shear stress on mitochondrial ATP generation, which is, to the best of our knowledge, the earliest mitochondrial response to shear stress exposure.

ECs release ATP in response to shear stress; in turn, the released ATP activates the P2X4 purinoceptors to cause cellular influx of extracellular Ca^{2+} (6, 38, 39). However, how ATP release is evoked by shear stress remains unknown. In the present study, we showed that shear stress caused the augmentation of mitochondrial ATP generation, and that blockade of mitochondrial ATP generation with inhibitors of the mitochondrial oxidative phosphorylation abolished the shear stress-induced ATP release. The treatment of ECs with 2-DG, an inhibitor of cytosolic glycolysis, had no effect on either the shear stress-induced ATP generation or the ATP release. These findings clearly indicated that the ATP released by shear stress originated from the mitochondria. Until recently, it has been assumed that ECs obtain most of their energy for their activities, including cell movement, cytoskeleton contraction, active transport of substances and ion channel opening from glycolysis, and that the primary functions of the mitochondria are the production of ROS and the mediation of redox signaling (27). This study is the first to demonstrate a novel role of mitochondria as mechanosignaling organelles that are able to transduce shear stress into ATP generation, triggering ATP release and purinoceptor-mediated Ca^{2+} signaling that lead to biological responses.

In previous studies, we demonstrated that shear stress induced highly concentrated, localized ATP release in the caveolae-rich regions of EC plasma membranes (37). Disruption of the caveolae using caveolin-1 siRNA or MβCD, which depletes membrane cholesterol, was found to abolish the localized ATP release, indicating that intact caveolae are a prerequisite for this release. Recently, it has become apparent that there are physical and functional interactions between the caveolae and mitochondria (28). Mitochondria have been observed in close contact with the plasma membrane in several mammalian cell types (19), including ECs, HeLa cells (17), hepatocytes (15), and cardiomyocytes (12, 34). For example, in HeLa cells, up to 10% of the total plasma membrane area is covered with mitochondria (known as sub-plasmalemmal mitochondria). Electron microscopy has demonstrated close apposition between mitochondria and the caveolae in cardiomyocytes, and that direct connections form between these organelles and membrane microdomains during ischemic stress (16). It is thought that the mitochondria located in close proximity to the caveolae supply them with highly concentrated ATP. There may be unidentified structures that link mitochondria to caveolae through which such ATP transfer can occur. Figure 5 shows a schematic diagram of the proposed caveolae-associated purinergic Ca^{2+} signaling in ECs exposed to shear stress.

Caveolins are localized in mitochondria as well as in the caveolae (16, 25). They can transfer

between the caveolae and mitochondria, which plays an important role in adaptation to cellular stress and injury. Caveolin-1 deficiency in mice has been shown to impair mitochondrial functions; it causes an accumulation of free cholesterol in the mitochondrial membranes, which increases membrane condensation and reduces the efficiency of the respiratory chain and intrinsic antioxidant defense, thereby increasing the cellular susceptibility to apoptosis (8). Loss of caveolin-1 also induces an increase in mitochondrial ROS and intracellular H_2O_2 production in the ECs (31). In the present study, we showed that knockdown of caveolin-1 with its siRNA abolished the shear stress-induced mitochondrial ATP generation. Although the functions of caveolin-1 localized in the mitochondria have not yet been clarified, it seems that caveolae or caveolins play a critical role in the shear stress-induced mitochondrial ATP generation.

ECs are known to respond to shear stress and increase the production of ROS in mitochondria as well as the Ca^{2+} concentration in both cytoplasm and mitochondria. These increased ROS and Ca^{2+} affect the mitochondrial ATP generation by modulating the activity of electron-transport chain and ATP synthase, whereas the produced ATP influences the ROS production and Ca^{2+} concentration. These mutual interplays among ROS, Ca^{2+} and ATP are thought to play an important role in maintaining EC homeostasis (1, 10). In the present study, we examined whether Ca^{2+} and ROS are involved in the shear-stress-induced mitochondrial ATP production and ATP release. Neither addition of EGTA to culture media, which removes extracellular Ca^{2+} and abolishes the shear-stress-induced Ca^{2+} influx, nor treatment of ECs with MitoTEMPOL, which inactivates mitochondrial ROS, exerted any influence on the shear-stress-induced ATP generation and ATP release. These findings indicate that the Ca^{2+} influx and ROS do not play a part in these events. On the other hand, not only the influx of extracellular Ca^{2+}, but also Ca^{2+} release from the endoplasmic reticulum (ER) also occurs in response to shear stress, and the mitochondria play an important role through Ca^{2+} uptake/release of the Ca^{2+} released by the ER (29). However, it remains unclear whether the Ca^{2+} released from the ER is related to the shear-stress-induced ATP production/ATP release.

At present, it remains unclear how shear stress causes augmented mitochondrial ATP generation in the ECs. Although as yet there is no direct evidence, several possible molecular mechanisms can be speculated. The first relates to the cytosolic pH level. Studies in rat and bovine aortic ECs have shown that cytosolic pH decreased within seconds of exposure to shear stress (26, 42, 43). This decrease appeared to be mediated by alterations in the functions of membrane ion transporters, such as the HCO_3^-/Cl^- and Na^+/H^+ exchangers. The decrease in pH (i.e., the increase in H^+ concentration) may in turn affect the activity of ATP synthase. Another possible mechanism relates to the O_2 concentration. In a recent study, we demonstrated that exposure of ECs to shear stress resulted in a reduction in the cholesterol content of their plasma membranes (36). Cholesterol acts as a barrier that limits the permeability of the lipid bilayer membrane of the cells to O_2 (14, 22, 32); thus, reduction of the

membrane cholesterol content increases the mitochondrial O_2 concentration, which may influence electron transfer chain reactions. A further possible mechanism involves the cytoskeletons. Mitochondria anchor to the cytoskeleton via actin-binding complexes in the outer membrane (7). Shear stress applied to the plasma membrane may be transmitted to the mitochondria via the cytoskeleton, affecting mitochondrial ATP generation. However, the biophysical process underlying the transduction of cytoskeletal strain to changes in mitochondrial functions remains unknown. It is possible that other factors may be implicated in the effects of shear stress on mitochondrial ATP generation, and further studies are needed to precisely elucidate the underlying mechanism.

ACKNOWLEDGMENTS

We wish to acknowledge Dr. Akira Kamiya and Dr. Kishio Furuya (Nagoya University) for their invaluable support in our work and thank Ms. Yuko Sawada for technical assistance.

GRANTS

This work was supported by Scientific Research from Japan Agency for Medical Research and Development (AMED) under Grant Number JP18gm0810006.

DISCLOSURES

The authors declare that they have no competing interests.

AUTHOR CONTRIBUTIONS

Both K.Y. and J.A. designed the study, conducted the experiments, analyzed the results, and wrote the manuscript. H.I. produced ATeam vector and purified AT1.03.

REFERENCES

1. **Alevriadou BR, Shanmughapriya S, Patel A, Stathopulos PB, and Madesh M**. Mitochondrial Ca^{2+} transport in the endothelium: regulation by ions, redox signalling and mechanical forces. *J R Soc Interface* 14: 2017.
2. **Anderson RG**. Plasmalemmal caveolae and GPI-anchored membrane proteins. *Curr Opin Cell Biol* 5: 647-652, 1993.
3. **Ando J, and Yamamoto K**. Flow detection and calcium signalling in vascular endothelial cells. *Cardiovasc Res* 99: 260-268, 2013.

4. **Ando J, and Yamamoto K**. Vascular mechanobiology: endothelial cell responses to fluid shear stress. *Circ J* 73: 1983-1992, 2009.
5. **Aoki T, Nishimura M, Matsuoka T, Yamamoto K, Furuyashiki T, Kataoka H, Kitaoka S, Ishibashi R, Ishibazawa A, Miyamoto S, Morishita R, Ando J, Hashimoto N, Nozaki K, and Narumiya S**. PGE_2 -EP_2 signalling in endothelium is activated by haemodynamic stress and induces cerebral aneurysm through an amplifying loop via NF-κB. *Br J Pharmacol* 163: 1237-1249, 2011.
6. **Bodin P, Bailey D, and Burnstock G**. Increased flow-induced ATP release from isolated vascular endothelial cells but not smooth muscle cells. *Br J Pharmacol* 103: 1203-1205, 1991.
7. **Boldogh I, Vojtov N, Karmon S, and Pon LA**. Interaction between mitochondria and the actin cytoskeleton in budding yeast requires two integral mitochondrial outer membrane proteins, Mmm1p and Mdm10p. *J Cell Biol* 141: 1371-1381, 1998.
8. **Bosch M, Mari M, Herms A, Fernandez A, Fajardo A, Kassan A, Giralt A, Colell A, Balgoma D, Barbero E, Gonzalez-Moreno E, Matias N, Tebar F, Balsinde J, Camps M, Enrich C, Gross SP, Garcia-Ruiz C, Perez-Navarro E, Fernandez-Checa JC, and Pol A**. Caveolin-1 deficiency causes cholesterol-dependent mitochondrial dysfunction and apoptotic susceptibility. *Curr Biol* 21: 681-686, 2011.
9. **Breton-Romero R, Acin-Perez R, Rodriguez-Pascual F, Martinez-Molledo M, Brandes RP, Rial E, Enriquez JA, and Lamas S**. Laminar shear stress regulates mitochondrial dynamics, bioenergetics responses and PRX3 activation in endothelial cells. *Biochim Biophys Acta* 1843: 2403-2413, 2014.
10. **Brookes PS, Yoon Y, Robotham JL, Anders MW, and Sheu SS**. Calcium, ATP, and ROS: a mitochondrial love-hate triangle. *Am J Physiol Cell Physiol* 287: C817-833, 2004.
11. **Chiu JJ, and Chien S**. Effects of disturbed flow on vascular endothelium: pathophysiological basis and clinical perspectives. *Physiol Rev* 91: 327-387, 2011.
12. **Csordas G, Varnai P, Golenar T, Roy S, Purkins G, Schneider TG, Balla T, and Hajnoczky G**. Imaging interorganelle contacts and local calcium dynamics at the ER-mitochondrial interface. *Mol Cell* 39: 121-132, 2010.
13. **Davies PF**. Flow-mediated endothelial mechanotransduction. *Physiol Rev* 75: 519-560, 1995.
14. **Dumas D, Latger V, Viriot ML, Blondel W, and Stoltz JF**. Membrane fluidity and oxygen diffusion in cholesterol-enriched endothelial cells. *Clin Hemorheol Microcirc* 21: 255-261, 1999.
15. **Fowler SL, Akins M, Zhou H, Figeys D, and Bennett SA**. The liver connexin32 interactome is a novel plasma membrane-mitochondrial signaling nexus. *J Proteome Res* 12: 2597-2610, 2013.
16. **Fridolfsson HN, Kawaraguchi Y, Ali SS, Panneerselvam M, Niesman IR, Finley JC, Kellerhals SE, Migita MY, Okada H, Moreno AL, Jennings M, Kidd MW, Bonds JA,**

Balijepalli RC, Ross RS, Patel PM, Miyanohara A, Chen Q, Lesnefsky EJ, Head BP, Roth DM, Insel PA, and Patel HH. Mitochondria-localized caveolin in adaptation to cellular stress and injury. *FASEB J* 26: 4637-4649, 2012.

17. **Frieden M, Arnaudeau S, Castelbou C, and Demaurex N**. Subplasmalemmal mitochondria modulate the activity of plasma membrane Ca^{2+}-ATPases. *J Biol Chem* 280: 43198-43208, 2005.
18. **Giedt RJ, Yang C, Zweier JL, Matzavinos A, and Alevriadou BR**. Mitochondrial fission in endothelial cells after simulated ischemia/reperfusion: role of nitric oxide and reactive oxygen species. *Free Radic Biol Med* 52: 348-356, 2012.
19. **Hutchinson TE, Kuchibhotla S, Block ER, and Patel JM**. Peptide-stimulation enhances compartmentalization and the catalytic activity of lung endothelial NOS. *Cell Physiol Biochem* 24: 471-482, 2009.
20. **Imamura H, Nhat KP, Togawa H, Saito K, Iino R, Kato-Yamada Y, Nagai T, and Noji H**. Visualization of ATP levels inside single living cells with fluorescence resonance energy transfer-based genetically encoded indicators. *Proc Natl Acad Sci U S A* 106: 15651-15656, 2009.
21. **Jones CI, 3rd, Han Z, Presley T, Varadharaj S, Zweier JL, Ilangovan G, and Alevriadou BR**. Endothelial cell respiration is affected by the oxygen tension during shear exposure: role of mitochondrial peroxynitrite. *Am J Physiol Cell Physiol* 295: C180-191, 2008.
22. **Khan N, Shen J, Chang TY, Chang CC, Fung PC, Grinberg O, Demidenko E, and Swartz H**. Plasma membrane cholesterol: a possible barrier to intracellular oxygen in normal and mutant CHO cells defective in cholesterol metabolism. *Biochemistry* 42: 23-29, 2003.
23. **Kim JS, Kim B, Lee H, Thakkar S, Babbitt DM, Eguchi S, Brown MD, and Park JY**. Shear stress-induced mitochondrial biogenesis decreases the release of microparticles from endothelial cells. *Am J Physiol Heart Circ Physiol* 309: H425-433, 2015.
24. **Kudo S, Morigaki R, Saito J, Ikeda M, Oka K, and Tanishita K**. Shear-stress effect on mitochondrial membrane potential and albumin uptake in cultured endothelial cells. *Biochem Biophys Res Commun* 270: 616-621, 2000.
25. **Li WP, Liu P, Pilcher BK, and Anderson RG**. Cell-specific targeting of caveolin-1 to caveolae, secretory vesicles, cytoplasm or mitochondria. *J Cell Sci* 114: 1397-1408, 2001.
26. **Patrick CW, and McIntire LV**. Fluid Shear Stress Effects on Endothelial Cell Cytosolic pH. *Tissue Eng* 1: 53-70, 1995.
27. **Quintero M, Colombo SL, Godfrey A, and Moncada S**. Mitochondria as signaling organelles in the vascular endothelium. *Proc Natl Acad Sci U S A* 103: 5379-5384, 2006.
28. **Ray S, Kassan A, Busija AR, Rangamani P, and Patel HH**. The plasma membrane as a capacitor for energy and metabolism. *Am J Physiol Cell Physiol* 310: C181-192, 2016.

29. **Scheitlin CG, Julian JA, Shanmughapriya S, Madesh M, Tsoukias NM, and Alevriadou BR**. Endothelial mitochondria regulate the intracellular Ca^{2+} response to fluid shear stress. *Am J Physiol Cell Physiol* 310: C479-490, 2016.
30. **Scheitlin CG, Nair DM, Crestanello JA, Zweier JL, and Alevriadou BR**. Fluid Mechanical Forces and Endothelial Mitochondria: A Bioengineering Perspective. *Cell Mol Bioeng* 7: 483-496, 2014.
31. **Shiroto T, Romero N, Sugiyama T, Sartoretto JL, Kalwa H, Yan Z, Shimokawa H, and Michel T**. Caveolin-1 is a critical determinant of autophagy, metabolic switching, and oxidative stress in vascular endothelium. *PLoS One* 9: e87871, 2014.
32. **Subczynski WK, Hyde JS, and Kusumi A**. Effect of alkyl chain unsaturation and cholesterol intercalation on oxygen transport in membranes: a pulse ESR spin labeling study. *Biochemistry* 30: 8578-8590, 1991.
33. **Takehara Y, Kanno T, Yoshioka T, Inoue M, and Utsumi K**. Oxygen-dependent regulation of mitochondrial energy metabolism by nitric oxide. *Arch Biochem Biophys* 323: 27-32, 1995.
34. **Wang J, Schilling JM, Niesman IR, Headrick JP, Finley JC, Kwan E, Patel PM, Head BP, Roth DM, Yue Y, and Patel HH**. Cardioprotective trafficking of caveolin to mitochondria is Gi-protein dependent. *Anesthesiology* 121: 538-548, 2014.
35. **Wang S, Iring A, Strilic B, Albarran Juarez J, Kaur H, Troidl K, Tonack S, Burbiel JC, Muller CE, Fleming I, Lundberg JO, Wettschureck N, and Offermanns S**. $P2Y_2$ and Gq/G_{11} control blood pressure by mediating endothelial mechanotransduction. *J Clin Invest* 125: 3077-3086, 2015.
36. **Yamamoto K, and Ando J**. Vascular endothelial cell membranes differentiate between stretch and shear stress through transitions in their lipid phases. *Am J Physiol Heart Circ Physiol* 309: H1178-1185, 2015.
37. **Yamamoto K, Furuya K, Nakamura M, Kobatake E, Sokabe M, and Ando J**. Visualization of flow-induced ATP release and triggering of Ca^{2+} waves at caveolae in vascular endothelial cells. *J Cell Sci* 124: 3477-3483, 2011.
38. **Yamamoto K, Korenaga R, Kamiya A, and Ando J**. Fluid shear stress activates Ca^{2+} influx into human endothelial cells via P2X4 purinoceptors. *Circ Res* 87: 385-391, 2000.
39. **Yamamoto K, Korenaga R, Kamiya A, Qi Z, Sokabe M, and Ando J**. $P2X_4$ receptors mediate ATP-induced calcium influx in human vascular endothelial cells. *Am J Physiol Heart Circ Physiol* 279: H285-292., 2000.
40. **Yamamoto K, Sokabe T, Matsumoto T, Yoshimura K, Shibata M, Ohura N, Fukuda T, Sato T, Sekine K, Kato S, Isshiki M, Fujita T, Kobayashi M, Kawamura K, Masuda H, Kamiya**

A, and Ando J. Impaired flow-dependent control of vascular tone and remodeling in P2X4-deficient mice. *Nat Med* 12: 133-137, 2006.

41. **Yamamoto K, Sokabe T, Ohura N, Nakatsuka H, Kamiya A, and Ando J**. Endogenously released ATP mediates shear stress-induced Ca^{2+} influx into pulmonary artery endothelial cells. *Am J Physiol Heart Circ Physiol* 285: H793-803, 2003.
42. **Ziegelstein RC, Blank PS, Cheng L, and Capogrossi MC**. Cytosolic alkalinization of vascular endothelial cells produced by an abrupt reduction in fluid shear stress. *Circ Res* 82: 803-809, 1998.
43. **Ziegelstein RC, Cheng L, and Capogrossi MC**. Flow-dependent cytosolic acidification of vascular endothelial cells. *Science* 258: 656-659, 1992.

FIGURE LEGENDS

Fig. 1. Monitoring of mitochondrial ATP levels in human pulmonary artery endothelial cells. A: distribution of the FRET-based ATP biosensor, mitAT1.03. This was correctly located in the mitochondria that were stained with MitoTracker Deep Red FM. The cell nuclei were stained with Hoechst 33342 and the cell margin obtained visualized under a phase contrast microscope was shown by a broken line. B: time course of the fluorescence intensity of cyan fluorescent protein (CFP; blue) and yellow fluorescent protein (YFP; red) inside the regions of interest. Treatment of the cells with an ATP synthase inhibitor oligomycin (10 μg/mL) induced a decrease in YFP intensity and an increase in CFP intensity. The YFP/CFP ratio therefore decreased, indicating a decrease in ATP levels. Treatment of the cells with an inhibitor of glycolysis (2-deoxy-D-glucose, 2-DG) (10 mM) had no effect on the YFP/CFP ratio. C: the ATP sensitivity of purified AT1.03. The plot of YFP/CFP ratios against Mg-ATP concentrations showed that the YFP/CFP ratio increased in an ATP concentration-dependent manner in the range of 0-10 mM. Oligomycin (10 μg/mL) had no effect on the ATP sensitivity of AT1.03.

Fig. 2. Effects of shear stress on the mitochondrial ATP levels. A: pseudocolor images of the yellow/cyan fluorescent protein (YFP/CFP) ratio before, during, and after the application of shear stress. The colors represent the ATP levels indicated by the scale. Shear stress (3 dynes/cm^2) increased ATP levels over the entire mitochondria. The time course of the YFP/CFP ratio showed that the ATP level rapidly increased in response to shear stress, remained at the increased level, and then returned to the control level after the shear stress ceased. B: response to the repeated application of shear stress. There was an increase in mitochondrial ATP level in response to each application of shear stress. Similar findings were observed in many cells. C: effects of hydrostatic pressure on the mitochondrial ATP levels. Hydrostatic pressure (40 mmHg) had no effect on ATP levels. In contrast, there was a marked increase in the ATP levels in response to shear stress. D: intensity-dependency of the shear stress-induced changes in mitochondrial ATP levels. ATP levels in the mitochondria increased further as the intensity of shear stress increased. E: bar graph showing the results of a quantitative analysis of the shear stress-induced changes in ATP levels. Values are means ± SD of the data obtained in 15 cells; $*P<0.05$, $**P<0.01$.

Fig. 3. Effects of inhibitors of glycolysis and the mitochondrial oxidative phosphorylation on the shear stress-induced increase in ATP generation. A: temporal changes in the mitochondrial ATP levels. Shear stress induced an increase in the ATP levels in the cells treated with the glycolysis inhibitor 2-deoxy-D-gllucose (2-DG, 10 mM), but not in the cells treated with an ATP synthase inhibitor (oligomycin, 10 μg/mL), a mitochondrial oxidative phosphorylation uncoupler (CCCP, 0.4 μg/mL), and a mitochondrial electron transport inhibitor (rotenone, 5 μM). This indicated that shear stress

activated the function of the mitochondrial oxidative phosphorylation. Neither addition of EGTA (1 mM) into culture medium that chelates extracellular Ca^{2+} nor treatment of ECs with MitoTEMPOL (50 μM) that inactivates mitochondrial ROS had an effect on the ATP generation. The baseline mitochondrial ATP concentrations were reduced by treatment of the ECs with oligomycin, CCCP or rotenone, while no such change was observed following treatment of the cells with 2-DG, EGTA or MitoTEMPOL. These mitochondrial ATP responses were representative of those of dozens of cells, all of which showed similar results. B: extracellular ATP release in response to shear stress. Human pulmonary artery endothelial cells (HPAECs) were exposed to shear stress (3 dynes/cm^2) for 1 min and the effluent was subjected to ATP measurement. The HPAECs released ATP in response to shear stress, and inhibitors of the mitochondrial oxidative phosphorylation (oligomycin, CCCP, and rotenone) markedly suppressed the ATP release, whereas a glycolysis inhibitor (2-DG), EGTA and MitoTEMPOL had no effect. Knockdown of caveolin-1 with its siRNA significantly suppressed the ATP release, whereas the scrambled siRNA had no effect. Results are presented as means ± SD of nine samples obtained in three separate experiments. *P<0.01 compared with the control.

Fig. 4. Involvement of caveolin-1 in the shear stress-induced ATP generation and Ca^{2+} signaling. A: relationship between mitochondria and caveolin-1, a marker protein for caveolae. After imaging mitochondria with MitoTracker Deep Red FM, the human pulmonary artery endothelial cells (HPAECs) were immunostained with an antibody to caveolin-1. The cell nuclei were stained with DAPI. Scrambled siCaveolin-1, cells transfected with a caveolin-1 scrambled siRNA; siCaveolin-1, cells transfected with a caveolin-1 siRNA. Caveolin-1 was unevenly distributed over the cell surface and was concentrated at a specific part of the cell periphery. The edge of the mitochondria was in close proximity to the region with concentrated caveolin-1. Caveolin-1 was completely knocked down by its siRNA. B: temporal changes in the mitochondrial ATP levels under shear stress. Shear stress increased mitochondrial ATP levels in the cells treated with a caveolin-1 scrambled siRNA, whereas caveolin-1 knockdown by its siRNA abolished the shear stress-induced mitochondrial ATP generation. These mitochondrial ATP responses were representative of those of dozens of cells, all of which showed similar results. C: Ca^{2+} responses to shear stress in HPAECs. Intracellular Ca^{2+} concentrations ($[Ca^{2+}]_i$) are expressed as the ratio of change in Fluo-4 fluorescence to the control before application of shear stress (F/F_0). The closed rectangles indicate the duration of shear stress (3 dynes/cm^2). Shear stress induced a marked increase in $[Ca^{2+}]_i$ in the cells treated with the caveolin-1 scrambled siRNA, but not in cells treated with caveolin-1 siRNA. Treatment of the cells with oligomycin (10 μg/mL), CCCP (0.4 μg/mL), or rotenone (5 μM) abolished the shear stress-mediated Ca^{2+} response. The Ca^{2+} response was blocked by EGTA (1 mM), but not by MitoTEMPOL (50 μM). No changes in the baseline intracellular concentrations were observed following treatment of the cells with any of the above inhibitors or

siRNA. Treatment of the cells withThese Ca^{2+}response curves are representative of those of dozens of cells, all of which showed similar results. These results indicated that caveolin-1 and mitochondrial ATP generation were implicated in the Ca^{2+} signaling following shear stress.

Fig.5. Schematic diagram of the proposed caveolae-associated purinergic Ca^{2+} signaling in ECs exposed to shear stress. Shear stress induces both diffuse ATP release from the entire surface of the cell membrane and a localized ATP release from the caveolae-rich cell regions. Since the localized ATP release reaches to more than 10 μM, it can activate the ATP-operated cation channel P2X4, thereby causing influx of extracellular Ca^{2+} into the cells. The increase in the intracellular Ca^{2+} concentration evokes a Ca^{2+} wave that starts at the caveolae and propagates throughout the entire cell. Mitochondria increase their ATP generation in response to shear stress exposure of the ECs and play a role as the source of the ATP released by the ECs. The mechanism underlying the induction of increased mitochondrial ATP generation in response to shear stress in the ECs remains unknown.

Figure 1

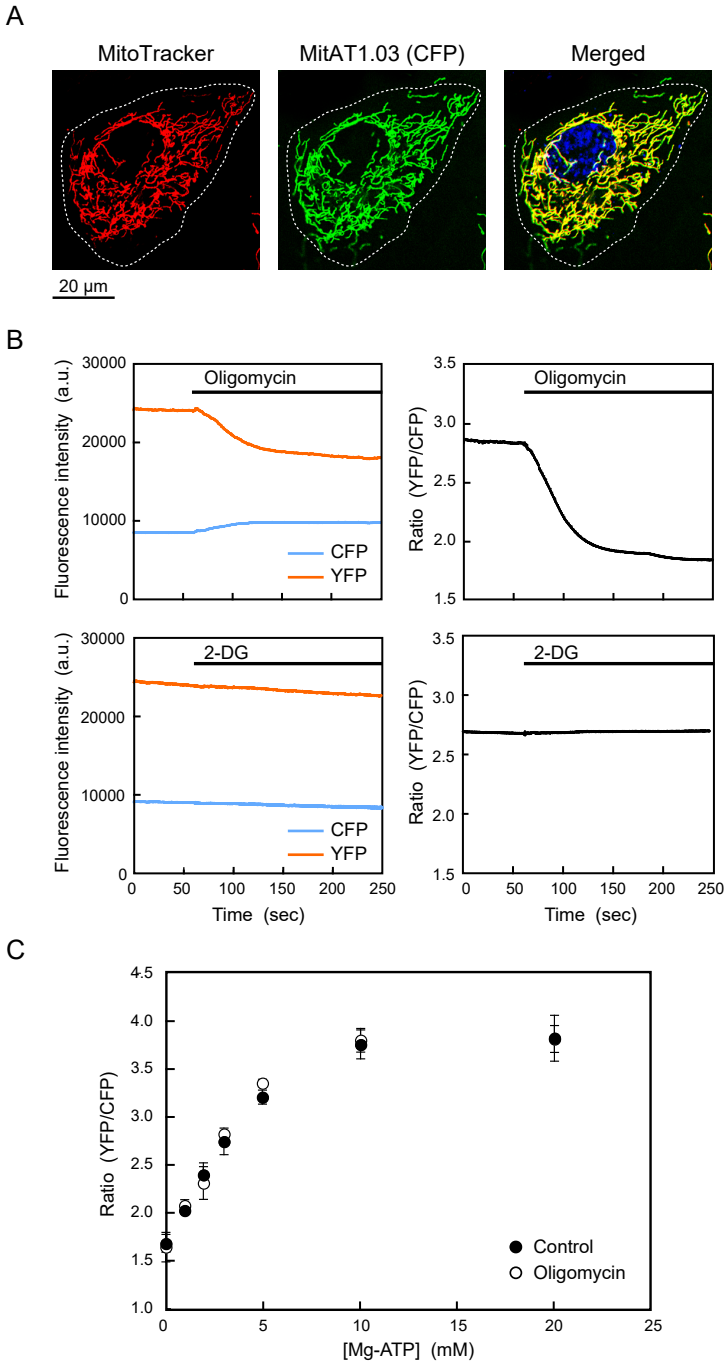

Figure 2

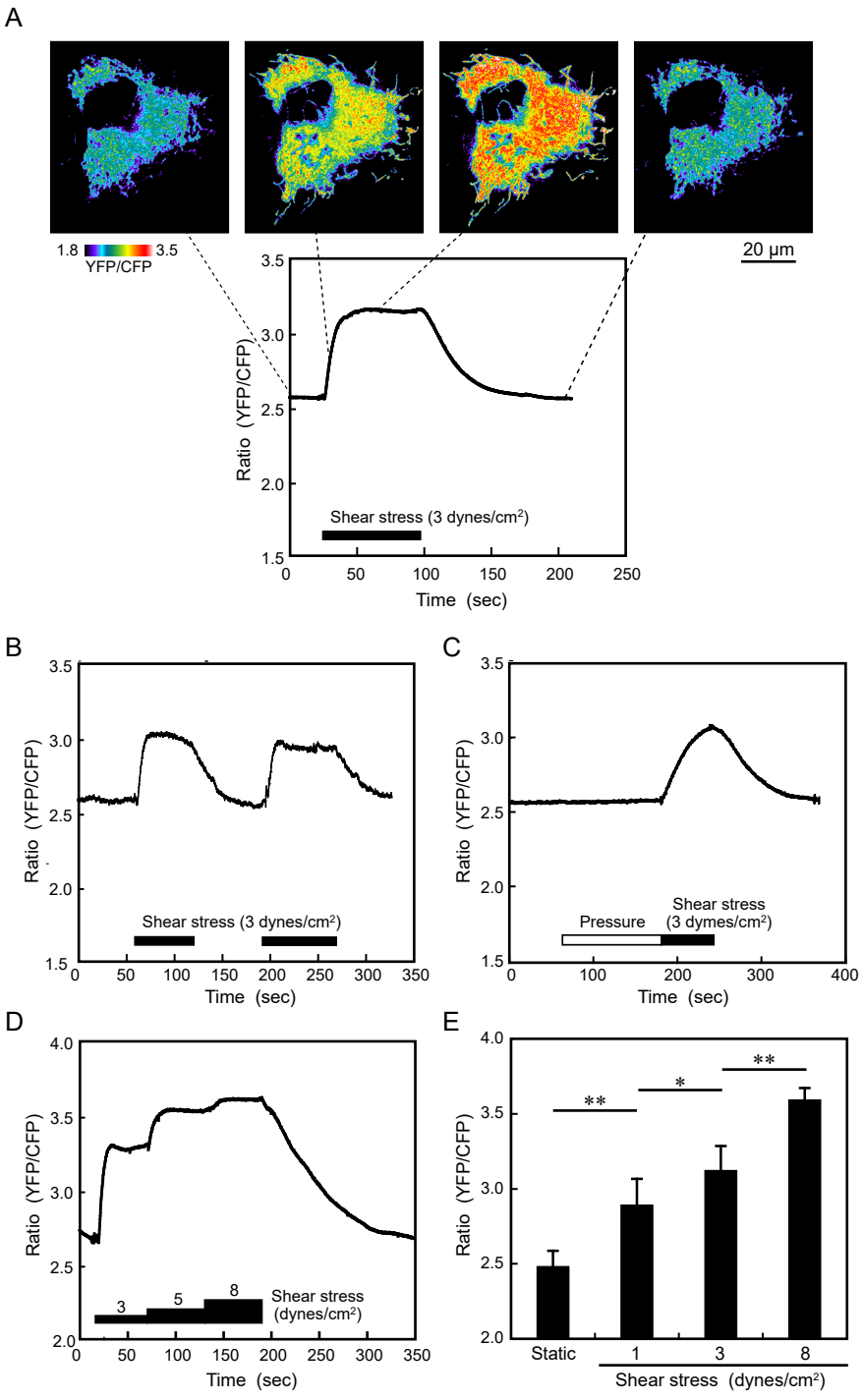

Figure 3

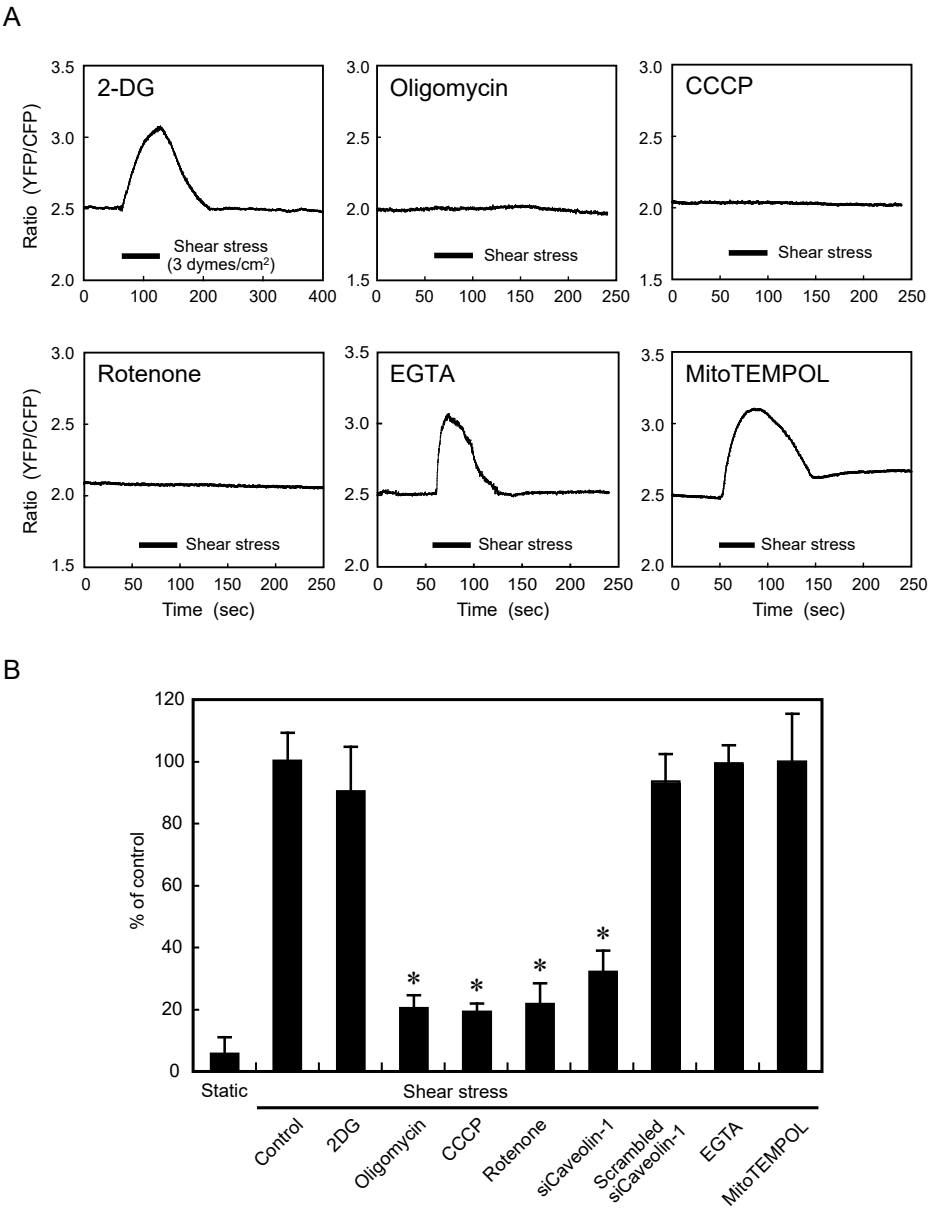

Figure 4

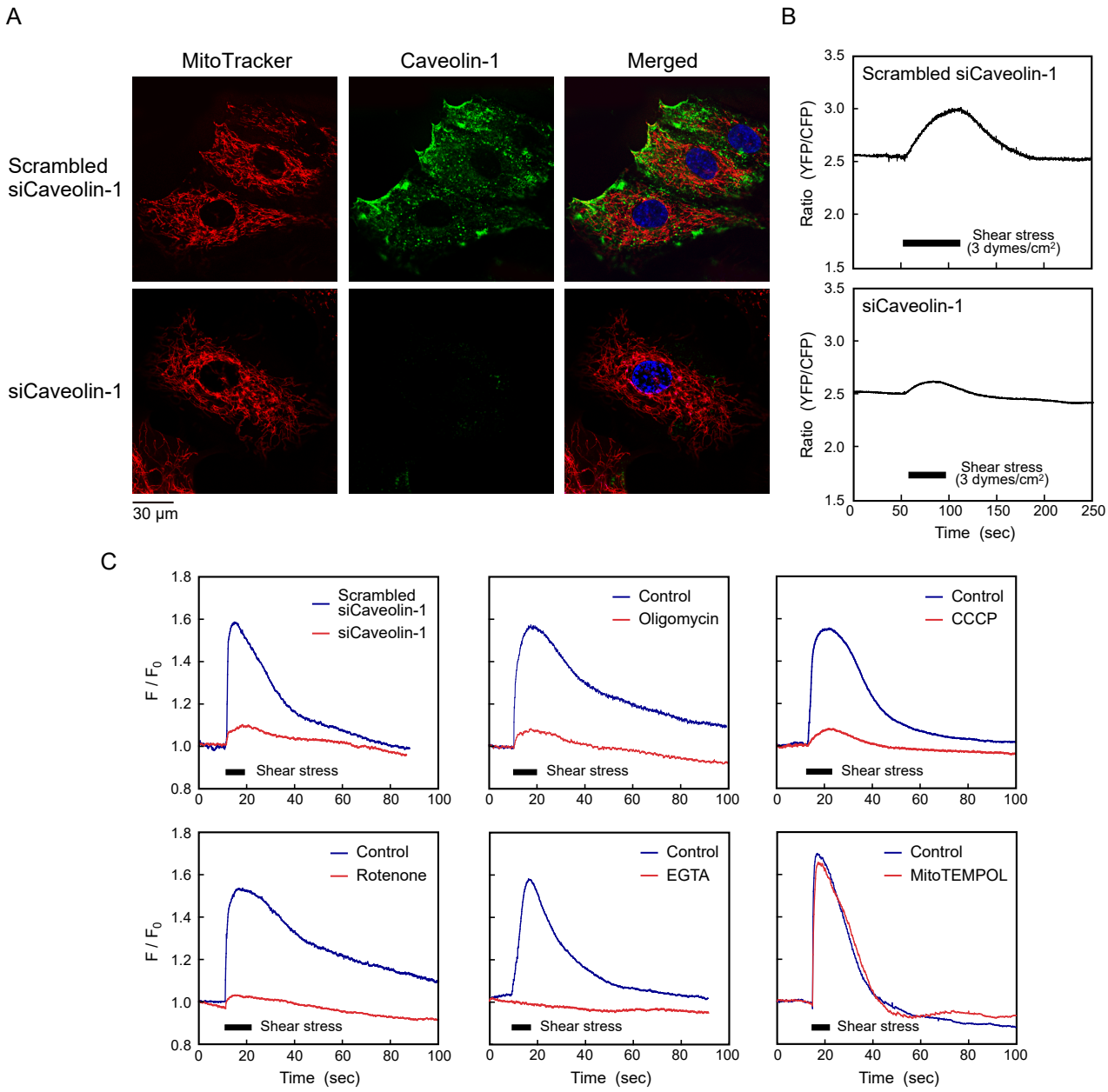

Figure 5